

This article was downloaded by:

On: 30 January 2011

Access details: Access Details: Free Access

Publisher Taylor & Francis

Informa Ltd Registered in England and Wales Registered Number: 1072954 Registered office: Mortimer House, 37-41 Mortimer Street, London W1T 3JH, UK



## Spectroscopy Letters

Publication details, including instructions for authors and subscription information:

<http://www.informaworld.com/smpp/title~content=t713597299>

### Tunable Upconversion Emissions from Lanthanide-doped Monodisperse $\beta$ -NaYF<sub>4</sub> Nanoparticles

Feng Wang<sup>a</sup>; Juan Wang<sup>a</sup>; Jun Xu<sup>b</sup>; Xuejia Xue<sup>a</sup>; Hongyu Chen<sup>b</sup>; Xiaogang Liu<sup>a</sup>

<sup>a</sup> Department of Chemistry, National University of Singapore, Singapore <sup>b</sup> Division of Chemistry & Biological Chemistry, Nanyang Technological University, Singapore

Online publication date: 30 July 2010

**To cite this Article** Wang, Feng , Wang, Juan , Xu, Jun , Xue, Xuejia , Chen, Hongyu and Liu, Xiaogang(2010) 'Tunable Upconversion Emissions from Lanthanide-doped Monodisperse  $\beta$ -NaYF<sub>4</sub> Nanoparticles', *Spectroscopy Letters*, 43: 5, 400 – 405

**To link to this Article: DOI:** 10.1080/00387010.2010.487018

**URL:** <http://dx.doi.org/10.1080/00387010.2010.487018>

## PLEASE SCROLL DOWN FOR ARTICLE

Full terms and conditions of use: <http://www.informaworld.com/terms-and-conditions-of-access.pdf>

This article may be used for research, teaching and private study purposes. Any substantial or systematic reproduction, re-distribution, re-selling, loan or sub-licensing, systematic supply or distribution in any form to anyone is expressly forbidden.

The publisher does not give any warranty express or implied or make any representation that the contents will be complete or accurate or up to date. The accuracy of any instructions, formulae and drug doses should be independently verified with primary sources. The publisher shall not be liable for any loss, actions, claims, proceedings, demand or costs or damages whatsoever or howsoever caused arising directly or indirectly in connection with or arising out of the use of this material.

# Tunable Upconversion Emissions from Lanthanide-doped Monodisperse $\beta$ -NaYF<sub>4</sub> Nanoparticles

Feng Wang<sup>1</sup>,  
Juan Wang<sup>1</sup>,  
Jun Xu<sup>2</sup>,  
Xuejia Xue<sup>1</sup>,  
Hongyu Chen<sup>2</sup>,  
and Xiaogang Liu<sup>1</sup>

<sup>1</sup>Department of Chemistry,  
National University of Singapore,  
Singapore

<sup>2</sup>Division of Chemistry &  
Biological Chemistry, Nanyang  
Technological University,  
Singapore

**ABSTRACT** We report upconversion multicolor tuning based on uniform  $\beta$ -NaYF<sub>4</sub>:Yb/Tm/Er nanoparticles. The as-synthesized nanoparticles with an average diameter of 25 nm are well dispersed in a wide range of nonpolar solvents including hexane, cyclohexane, dichloromethane, and toluene. These nanoparticles show intense upconversion emissions and the color output can be precisely modulated by adjusting activator ratios of Tm<sup>3+</sup> to Er<sup>3+</sup>. Dopant-concentration dependent emission properties of the triply doped particle system are also investigated. In addition, we demonstrate that these nanoparticles can be readily transferred to polar solvents such as ethanol and water by growing a thin silica layer (10 nm) around the particles, providing potential applications in biological labeling and imaging.

**KEYWORDS** energy transfer, lanthanide, multicolor tuning, NaYF<sub>4</sub>, silica coating, upconversion

## 1. INTRODUCTION

The ability to manipulate color output of luminescent nanomaterials with reference to human visual systems is extremely useful in understanding the underlying luminescence mechanism of these nanomaterials and in exploring their applications as light emitting displays, lasers, and optoelectronic devices to multiplexed biological labeling.<sup>[1–3]</sup> A general approach to tuning emission colors is based on controlling emission wavelength of the nanomaterials, such as quantum dots and rare-earth nanocrystals. For example, the emission wavelength of the quantum dots depends on dot size. Smaller quantum dots generally exhibit shorter emission wavelengths. Thus, a wide spectrum of emission colors can be readily produced by using a set of variable sized quantum dots.<sup>[4,5]</sup> A complementary approach to color manipulation is to control the relative emission intensities of the nanomaterials by varying material compositions or dopant concentrations.<sup>[6–9]</sup> In stark contrast to quantum dots, lanthanide-doped nanoparticles typically exhibit large Stokes shifts and a distinct set of sharp emission bands arising from f-f electronic transitions.<sup>[10,11]</sup> The emission colors of these lanthanide-doped nanoparticles can be tuned by controlling either emission wavelength or

Received 27 July 2009;  
accepted 10 September 2009.

Address correspondence to  
Xiaogang Liu, Department of  
Chemistry, National University of  
Singapore, 3 Science Drive 3,  
Singapore 117543. E-mail:  
chmlx@nus.edu.sg

relative emission intensities.<sup>[6,7]</sup> Despite the recent advance in multicolor emission tuning, most of these approaches have significant limitations imposed by autofluorescence and optical photodamage problems due to excitation in the ultraviolet or blue spectral region.

Alternatively, visible emission can be generated by near-infrared (NIR) excitation of lanthanide-doped nanomaterials in a unique process known as upconversion.<sup>[12–14]</sup> Compared to conventional downconversion luminescent counterparts, upconversion nanomaterials offer high photochemical stability, large anti-Stokes shifts, and absence of autofluorescence in biological samples under infrared excitation.<sup>[14]</sup> Once surface-functionalized and dispersed in aqueous solutions, these upconversion nanomaterials are ideal luminescent probes in biological labeling and imaging studies.<sup>[15–20]</sup> Although photon upconversion processes can be expected for all lanthanides, practically useful NIR to visible upconversion only occurs in the presence of a limited number of lanthanide activators.<sup>[21]</sup> In particular, the most efficient upconversion nanoparticles known to date are obtained with  $\text{Er}^{3+}$  and  $\text{Tm}^{3+}$  as the activators, in conjunction with  $\text{Yb}^{3+}$  as the sensitizer.<sup>[14]</sup> Manipulation of multicolor upconversion emissions in the nanoparticles is primarily based on controlling relative emission intensities of  $\text{Er}^{3+}$  and  $\text{Tm}^{3+}$  through precise control of host/dopant combination,<sup>[22–27]</sup> dopant concentration,<sup>[28–31]</sup> and physical size of the host.<sup>[32,33]</sup>

Recently, we demonstrated a general and versatile approach to fine-tuning the upconversion emission colors, based upon a single host source of  $\alpha\text{-NaYF}_4$  (or cubic phase  $\text{NaYF}_4$ ) nanoparticles doped with  $\text{Yb}^{3+}$ ,  $\text{Tm}^{3+}$ , and  $\text{Er}^{3+}$ .<sup>[29]</sup> By precise control of the emission intensity balance through control of different combinations of lanthanide dopants and dopant concentration, the luminescence emission can be tuned from visible to NIR under single-wavelength excitation. Here, we show that the scope of the approach can be extended to  $\beta\text{-NaYF}_4$  (or hexagonal phase  $\text{NaYF}_4$ ) nanoparticles that are known to offer about an order of magnitude enhancement of upconversion efficiency relative to its cubic phase counterpart. Multicolor emission tuning is achieved through doping  $\text{Yb}/\text{Tm}/\text{Er}$  at controlled dopant concentrations. We also report the silica coating of these lanthanide-doped nanoparticles.

## 2. EXPERIMENTAL SECTION

### 2.1. Materials

$\text{YCl}_3\bullet6\text{H}_2\text{O}$  (99.99%),  $\text{YbCl}_3\bullet6\text{H}_2\text{O}$  (99.99%),  $\text{ErCl}_3\bullet6\text{H}_2\text{O}$  (99.9%),  $\text{TmCl}_3\bullet6\text{H}_2\text{O}$  (99.99%),  $\text{NaOH}$  (98 + %),  $\text{NH}_4\text{F}$  (98 + %), 1-octadecene (90%), oleic acid (90%), tetraethyl orthosilicate (TEOS, 98%), and polyoxyethylene (5) nonylphenylether (IGEPAL® CO-520) were purchased from Sigma-Aldrich and used as starting materials without further purification.

### 2.2. Nanoparticle Synthesis

In a typical experiment, 2 mL solutions of  $\text{RECl}_3$  (0.2 M, RE=Y, Yb, Er, and Tm) in methanol were added to a 50 mL flask containing 3 mL of oleic acid and 7 mL of 1-octadecene. The solution was heated to 160°C for 30 min and then cooled to room temperature. Subsequently, a 5 mL methanol solution of  $\text{NH}_4\text{F}$  (1.6 mmol) and  $\text{NaOH}$  (1 mmol) was added to the flask and the resulting mixture was stirred for 30 min. After removal of the methanol by evaporation, the solution was heated to 300°C under argon for 1.5 h and cooled to room temperature. The resulting nanoparticles were precipitated by addition of ethanol, collected by centrifugation, washed with water and ethanol for several times, and re-dispersed in cyclohexane.

### 2.3. Silica Coating

In a typical experiment, 0.1 mL of CO-520 and 10 mL of cyclohexane containing 0.04-mmol  $\text{NaYF}_4$  nanoparticles were mixed and stirred for 10 min. Then 0.4 mL of CO-520 and 0.1 mL of ammonia (wt. 25%) were added and the container was sealed and sonicated for 20 min to form a transparent emulsion. To the emulsion was then added 0.04 mL of TEOS and the resulting mixture was stirred for 2 days. Silica-coated  $\text{NaYF}_4$  nanoparticles were precipitated by adding acetone, washed with ethanol and water, and then stored in water.

### 2.4. Characterizations

X-ray diffraction (XRD) analysis was carried out on a Siemens D5005 X-ray diffractometer with  $\text{Cu K}\alpha$  radiation ( $\lambda=1.5406\text{\AA}$ ). Transmission electron microscopic measurements were carried out on a

JEOL 2010 transmission electron microscope operating at an acceleration voltage of 200 kV. The luminescence spectra were obtained with a DM150i monochromator equipped with a R928 photon counting photomultiplier tube (PMT), in conjunction with a 980 nm diode laser. All luminescence studies were carried out at room temperature.

### 3. RESULTS AND DISCUSSION

The size and morphology of the as-prepared  $\text{NaYF}_4$ :Yb/Tm (20/0.2 mol %) nanoparticles were studied by transmission electron microscopy (TEM). As shown in Figure 1a, the nanoparticles exhibit a spherical shape with a uniform diameter of 25 nm. Passivated by oleic acid ligand, the nanoparticles are well dispersed in nonpolar solvents such as hexane, cyclohexane, dichloromethane, and toluene. Because of the high size-monodispersity, these nanoparticles easily self-assembled on the copper grids upon drying, forming ordered layer lattices (Figure 1b). The sample was further studied by XRD and all peaks in the pattern shown in Figure 1c can be well indexed in accordance with hexagonal phase  $\text{NaYF}_4$  crystal (JCPDS file no. 16-0334), indicating pure hexagonal phase of the nanoparticles. Hexagonal phase  $\text{NaYF}_4$  (space group  $P6_3/m$ ) contains two cation sites: one occupied by Na and the other occupied randomly by Na and Y (Figure 1c, inset). The point symmetry of lanthanide site in the hexagonal phase is  $C_{3h}$ , lower than the  $O_h$  symmetry in the cubic phase. The low point symmetry allows intermixing of the f states of the lanthanide dopant ions with higher electronic configuration, which lifts the parity selection rule and subsequently increases f-f transition probability.<sup>[14]</sup> Thus, upconversion efficiency of the hexagonal phase is higher than that of the cubic phase counterpart.

Figure 2 shows room-temperature upconversion emission spectra of the  $\text{NaYF}_4$  nanoparticles triply-doped with Yb/Tm/Er at controlled dopant concentrations. The Yb/Tm co-doped  $\text{NaYF}_4$  exhibits a blue color emission resulting from  $^1\text{D}_2 \rightarrow ^3\text{F}_4$  (450 nm),  $^1\text{G}_4 \rightarrow ^3\text{H}_6$  (475 nm), and  $^1\text{G}_4 \rightarrow ^3\text{F}_4$  (650 nm) transitions of  $\text{Tm}^{3+}$ . By adding  $\text{Er}^{3+}$  ions into the system, characteristic emission peaks corresponding to  $^2\text{H}_{9/2} \rightarrow ^4\text{I}_{15/2}$  (410 nm),  $^2\text{H}_{11/2}$ ,  $^4\text{S}_{3/2} \rightarrow ^4\text{I}_{15/2}$  (525 and 540 nm), and  $^4\text{F}_{9/2} \rightarrow ^4\text{I}_{15/2}$  (660 nm) transitions of  $\text{Er}^{3+}$  were observed. By increasing the dopant concentration

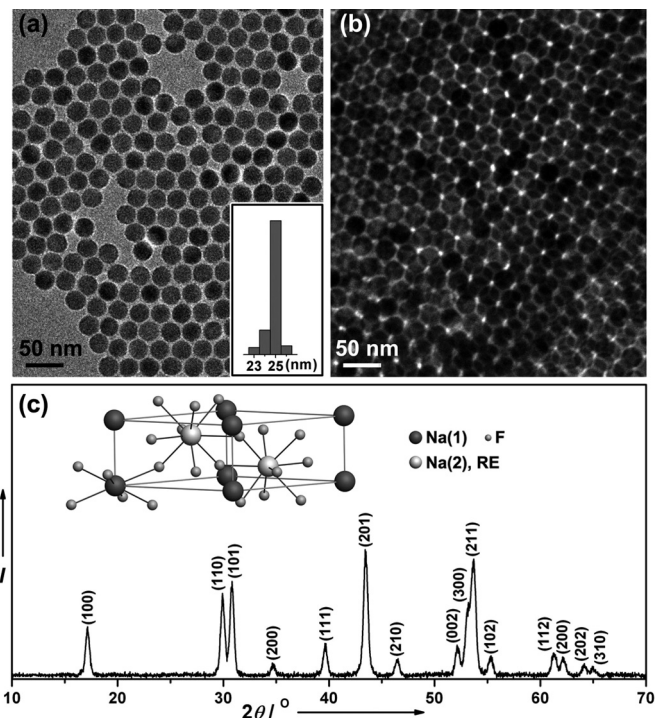


**FIGURE 1** TEM image showing self-assembled (a) monolayer (Inset: histogram showing size distribution of the nanoparticles) and (b) double layer of the as-synthesized  $\text{NaYF}_4$ :Yb/Tm nanoparticles. (c) XRD pattern of the corresponding sample (Inset: schematic presentation of hexagonal phase  $\text{NaYF}_4$  structure consisting of an ordered array of F ions with two types of cation sites selectively occupied by Na and Y ions). Note the triply-doped nanoparticles exhibit essentially the same morphology, size, and crystal phase as the Yb/Tm co-doped nanoparticles.

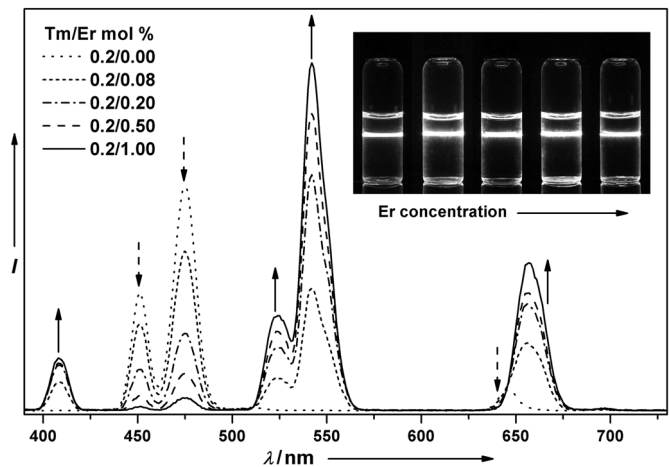


**FIGURE 2** Room-temperature upconversion emission spectra of  $\text{NaYF}_4$ :Yb/Tm/Er (20/0.2/0–1 mol %) nanoparticles dispersed in cyclohexane solutions. The  $\text{Tm}^{3+}$  and  $\text{Er}^{3+}$  emissions were marked by dash and solid arrows, respectively (Inset: luminescent photos showing multicolor emissions of the samples with varied  $\text{Er}^{3+}$  dopant concentrations). The samples were excited with a 980 nm diode laser operating at 600 mW.

of  $\text{Er}^{3+}$ , the relative intensity ratio of  $\text{Er}^{3+}$  to  $\text{Tm}^{3+}$  can be precisely controlled, resulting in a tunable color output. It should be mentioned that the emission intensity ratio of  $\text{Tm}^{3+}$  to  $\text{Er}^{3+}$  is much lower than that previously observed for  $\text{Yb}/\text{Tm}/\text{Er}$  triply-doped cubic phase  $\text{NaYF}_4$  with the same dopant concentrations.<sup>[29]</sup> We attribute the different optical properties to the dissimilar nanocrystal structures and different types of surface-tethered ligands, both of which have significant impact on luminescence behavior of the dopant ions. For example, oleic acid quenches lanthanide luminescence more efficiently than polyethylenimine due to the presence of high energy  $\text{C}=\text{O}$  oscillator.

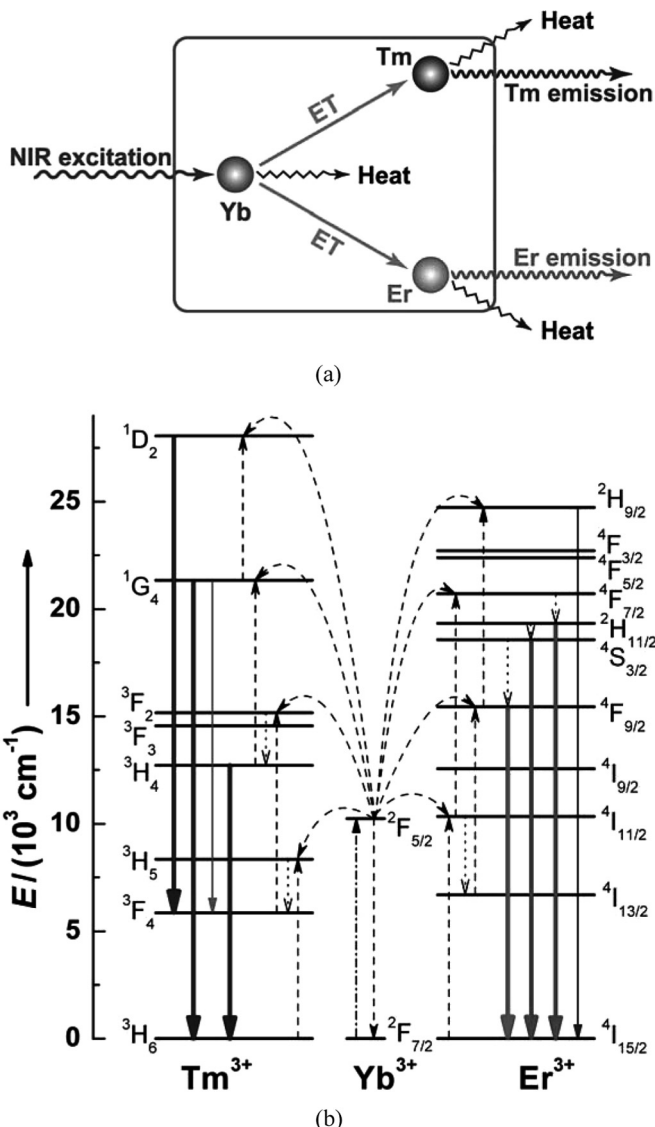


**FIGURE 3** (a) Schematic illustration showing the proposed optical processes in  $\text{Yb}/\text{Tm}/\text{Er}$  triply-doped  $\text{NaYF}_4$  nanoparticles under  $980\text{ nm}$  excitation. (b) Energy level diagram showing the proposed mechanism of energy transfer from  $\text{Yb}^{3+}$  to  $\text{Tm}^{3+}$  and  $\text{Er}^{3+}$ .

The un-normalized spectra in Figure 2 clearly indicate that the  $\text{Tm}^{3+}$  emission intensities decrease rapidly with increasing  $\text{Er}^{3+}$  dopant concentration. This result is primarily due to different energy transfer (ET) processes in the triply-doped system compared to its  $\text{Yb}/\text{Tm}$  co-doped counterpart. Figure 3a shows proposed optical processes in the  $\text{Yb}/\text{Tm}/\text{Er}$  triply-doped  $\text{NaYF}_4$  nanoparticles. The  $\text{Tm}^{3+}$  and  $\text{Er}^{3+}$  are activators that produce the upconversion emissions.  $\text{Yb}^{3+}$  is the sensitizer that absorbs the NIR excitations and then transfers its energy to the activators (Figure 3b). Due to its larger absorption cross-section as well as efficient energy transfer to most upconverting lanthanide ions,  $\text{Yb}^{3+}$  can significantly enhance the upconversion emissions of lanthanide activators. In contrast to single-activator system, the sensitizer  $\text{Yb}^{3+}$  will transfer its absorbed excitation energy to both  $\text{Tm}^{3+}$  and  $\text{Er}^{3+}$ . At elevated concentrations of  $\text{Er}^{3+}$ , the excitation energy absorbed by  $\text{Yb}^{3+}$  is predominantly transferred to  $\text{Er}^{3+}$ , resulting in suppressed emission intensities of  $\text{Tm}^{3+}$ .

In a previous work, Zhang and a co-worker<sup>[30]</sup> suggested that energy transfer from  $\text{Tm}^{3+}$  to  $\text{Er}^{3+}$  may occur, resulting in an increase in the  $\text{Er}^{3+}$  emission intensity and a decrease in the  $\text{Tm}^{3+}$  emission intensity. However, the energy transfer between  $\text{Tm}^{3+}$  and  $\text{Er}^{3+}$  is unlikely to occur in our particle system. As a control experiment, we prepared a sample of  $\text{NaYF}_4:\text{Yb}/\text{Er}$  (20/1 mol%) and compared its emission spectrum with that of  $\text{NaYF}_4:\text{Yb}/\text{Er}/\text{Tm}$  (20/1/0.2 mol%). As shown in Fig. 4, the addition

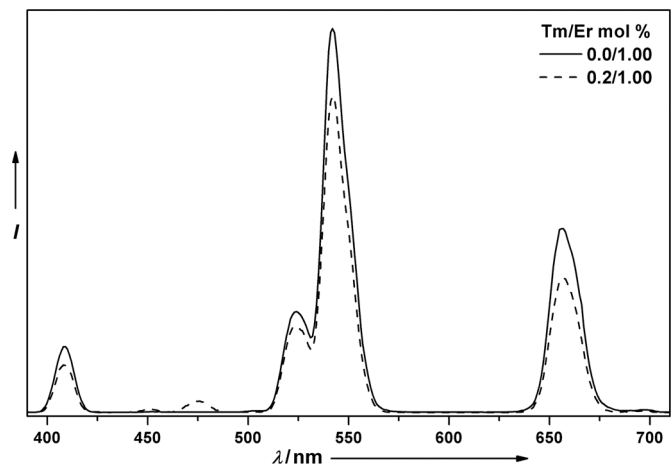


**FIGURE 4** Room-temperature upconversion emission spectra of  $\text{NaYF}_4:\text{Yb}/\text{Tm}/\text{Er}$  (20/0–0.2/1 mol%) nanoparticles dispersed in cyclohexane solutions. The samples were excited with a 980 nm diode laser operating at 600 mW.

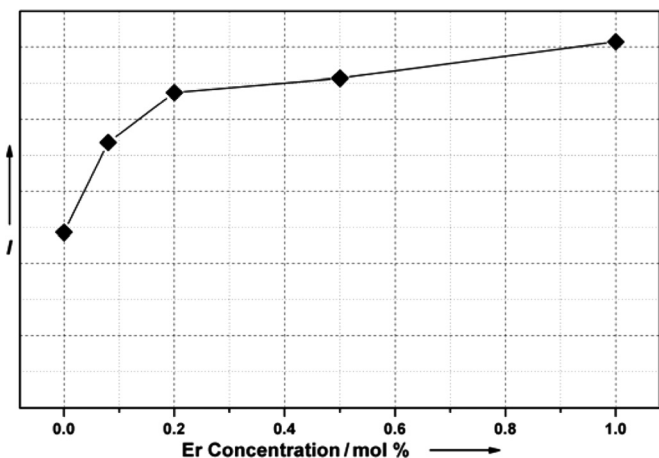


**FIGURE 5** Integrated upconversion emission intensities of the  $\text{NaYF}_4\text{:Yb/Tm/Er}$  ( $20/0.2/x$  mol %) nanoparticles as a function of dopant concentration of  $\text{Er}^{3+}$ .

of  $\text{Tm}^{3+}$  into the  $\text{NaYF}_4\text{:Yb/Er}$  nanoparticles leads to a decrease in the  $\text{Er}^{3+}$  emission intensity, which can be attributed to partial excitation energy transfer from  $\text{Yb}^{3+}$  to  $\text{Tm}^{3+}$ . In addition, we further investigated the overall emission intensities of the samples at different  $\text{Er}^{3+}$  dopant concentrations. We found that there was no quenching effect occurred with increasing  $\text{Er}^{3+}$  dopant concentrations up to 1 mol % (Fig. 5). Thus, the possibility of energy loss through cross-relaxation between  $\text{Tm}^{3+}$  and  $\text{Er}^{3+}$  was further excluded. It should be noted that the lanthanide luminescence is strongly dependent on the dopant concentration. At higher dopant

concentrations of  $\text{Tm}^{3+}$  and  $\text{Er}^{3+}$ , significant energy loss may occur due to enhanced cross-relaxation arising from decreased dopant-dopant interionic distance.

Stabilized by oleic acid ligands, the as-synthesized  $\text{NaYF}_4$  nanoparticles exhibit high dispersibility in various non-polar solvents including hexane, cyclohexane, dichloromethane, and toluene. More importantly, these triply doped upconversion nanoparticles can be surface-modified to provide hydrophilic wetting properties. As a proof-of-concept experiment, the luminescent nanoparticles dispersed in cyclohexane were transferred into an aqueous solution and subsequently coated with a thin layer of silica using a reverse microemulsion method.<sup>[34–36]</sup> Figure 6 shows a representative TEM image of the highly uniform silica-coated nanoparticles with an average diameter of 45 nm.

## 4. CONCLUSIONS

In conclusion, we have reported the synthesis of lanthanide-doped monodisperse hexagonal-phase  $\text{NaYF}_4$  nanoparticles. The as-synthesized nanoparticles dispersed in non-polar solvents can be readily transferred to polar solvent through silica coating. Importantly, the simultaneous doping of two types of activators ( $\text{Tm}^{3+}$  and  $\text{Er}^{3+}$ ) into the host lattice has no deleterious (or quenching) effects on the upconversion emission of the nanoparticles, while allowing for deliberate tuning of the output color. Due to their small feature size, high dispersibility in a wide variety of solvents as well as tunable upconversion emissions, these nanoparticles should hold great promise for practical applications ranging from multiplex biological labeling to solid state lighting.<sup>[37–41]</sup>

## ACKNOWLEDGMENTS

This study was supported by NUS Academic Research Fund (Grant Nos. R-143-000-317 and R-143-000-342) and a Young Investigator Award (Grant No. R-143-000-318) to X.L. by NUS.

## REFERENCES

1. Bruchez, M.; Moronne, M.; Gin, P.; Weiss, S.; Alivisatos, A. P. Semiconductor nanocrystals as fluorescent biological labels. *Science* 1998, 281, 2013–2016.
2. Wang, F.; Tan, W. B.; Zhang, Y.; Fan, X. P.; Wang, M. Q. Luminescent nanomaterials for biological labelling. *Nanotechnology* 2006, 17, R1–R13.

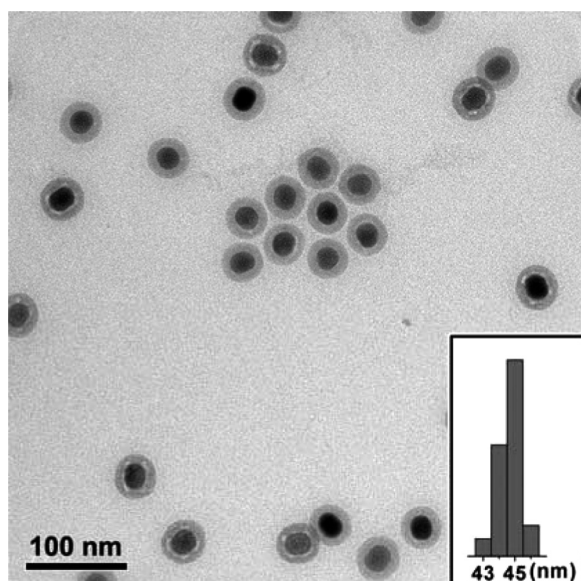


**FIGURE 6** TEM image of the silica-coated  $\text{NaYF}_4\text{:Yb/Tm/Er}$  ( $20/0.2/0.08$  mol %) nanoparticles (Inset: histogram showing size distribution of the silica-coated upconversion nanoparticles).

3. Jiang, C.; Wang, F.; Wu, N.; Liu, X. Up- and down-conversion cubic zirconia and hafnia nanobelts. *Adv. Mater.* **2008**, *20*, 4826–4829.
4. Murray, C. B.; Norris, D. J.; Bawendi, M. G. Synthesis and characterization of nearly monodisperse CdE (E=S, Se, Te) semiconductor nanocrystallites. *J. Am. Chem. Soc.* **1993**, *115*, 8706–8715.
5. Cao, Y. C.; Wang, J. One-pot synthesis of high-quality zinc-blende CdS nanocrystals. *J. Am. Chem. Soc.* **2004**, *126*, 14336–14337.
6. Wang, F.; Fan, X. P.; Wang, M. Q.; Zhang, Y. Multicolour PEI/NaGdF<sub>4</sub>:Ce<sup>3+</sup>,Ln<sup>3+</sup> nanocrystals by single-wavelength excitation. *Nanotechnology* **2007**, *18*, 025701.
7. Wang, F.; Xue, X.; Liu, X. Multicolor tuning of (Ln, P)-Doped YVO<sub>4</sub> nanoparticles by single-wavelength excitation. *Angew. Chem. Int. Ed.* **2008**, *47*, 906–909.
8. Han, M.; Gao, X.; Su, J.; Nie, S. Quantum-dot-tagged microbeads for multiplexed optical coding of biomolecules. *Nat. Biotechnol.* **2001**, *19*, 631–635.
9. Wang, L.; Tan, W. H. Multicolor FRET silica nanoparticles by single wavelength excitation. *Nano Lett.* **2006**, *6*, 84–88.
10. Wong, H.-T.; Chan, H. L. W.; Hao, J. H. Magnetic and luminescent properties of multifunctional GdF<sub>3</sub>:Eu<sup>3+</sup> nanoparticles. *Appl. Phys. Lett.* **2009**, *95*, 022512.
11. Luo, W.; Li, R.; Chen, X. Host-sensitized luminescence of Nd<sup>3+</sup> and Sm<sup>3+</sup> ions incorporated in anatase titania nanocrystals. *J. Phys. Chem. C* **2009**, *113*, 8772–8777.
12. Auzel, F. Upconversion and anti-stokes processes with f and d ions in solids. *Chem. Rev.* **2004**, *104*, 139–173.
13. Suyver, J. F.; Aebsicher, A.; Biner, D.; Gerner, P.; Grimm, J.; Heer, S.; Krämer, K. W.; Reinhard, C.; Güdel, H. U. Novel materials doped with trivalent lanthanides and transition metal ions showing near-infrared to visible photon upconversion. *Opt. Mater.* **2005**, *27*, 1111–1130.
14. Wang, F.; Liu, X. Recent advances in the chemistry of lanthanide-doped upconversion nanocrystals. *Chem. Soc. Rev.* **2009**, *38*, 976–989.
15. van de Rijke, F.; Zijlmans, H.; Li, S.; Vail, T.; Raap, A. K.; Niedbala, R. S.; Tanke, H. J. Up-converting phosphor reporters for nucleic acid microarrays. *Nat. Biotech.* **2001**, *19*, 273–276.
16. Wang, L. Y.; Yan, R. X.; Hao, Z. Y.; Wang, L.; Zeng, J. H.; Bao, H.; Wang, X.; Peng, Q.; Li, Y. D. Fluorescence resonant energy transfer biosensor based on upconversion-luminescent nanoparticles. *Angew. Chem. Int. Ed.* **2005**, *44*, 6054–6057.
17. Nyk, M.; Kumar, R.; Ohulchansky, T. Y.; Bergey, E. J.; Prasad, P. N. High contrast in vitro and in vivo photoluminescence bioimaging using near infrared to near infrared up-conversion in Tm<sup>3+</sup> and Yb<sup>3+</sup> doped fluoride nanophosphors. *Nano Lett.* **2008**, *8*, 3834–3838.
18. Chen, Z.; Chen, H.; Hu, H.; Yu, M.; Li, F.; Zhang, Q.; Zhou, Z.; Yi, T.; Huang, C. Versatile synthesis strategy for carboxylic acid-functionalized upconverting nanophosphors as biological labels. *J. Am. Chem. Soc.* **2008**, *130*, 3023–3029.
19. Hu, H.; Xiong, L.; Zhou, J.; Li, F.; Cao, T.; Huang, C. Multimodal-luminescence core-shell nanocomposites for targeted imaging of tumor cells. *Chem. Eur. J.* **2009**, *15*, 3577–3584.
20. Wu, S. W.; Han, G.; Milliron, D. J.; Aloni, S.; Altoe, V.; Talapin, D. V.; Cohen, B. E.; Schuck, P. J. Non-blinking and photostable upconverted luminescence from single lanthanide-doped nanocrystals. *Proc. Natl. Acad. Sci. USA* **2009**, *106*, 10917–10921.
21. Ehlert, O.; Thomann, R.; Darbandi, M.; Nann, T. A four-color colloidal multiplexing nanoparticle system. *ACS Nano* **2008**, *2*, 120–124.
22. Heer, S.; Lehmann, O.; Haase, M.; Güdel, H. U. Blue, green, and red upconversion emission from lanthanide-doped LuPO<sub>4</sub> and YbPO<sub>4</sub> nanocrystals in a transparent colloidal solution. *Angew. Chem. Int. Ed.* **2003**, *42*, 3179–3182.
23. Heer, S.; Kömpe, K.; Güdel, H. U.; Haase, M. Highly efficient multicolour upconversion emission in transparent colloids of lanthanide-doped NaYF<sub>4</sub> nanocrystals. *Adv. Mater.* **2004**, *16*, 2102–2105.
24. Yi, G. S.; Chow, G. M. Synthesis of hexagonal-phase NaYF<sub>4</sub>:Yb,Er and NaYF<sub>4</sub>:Yb,Tm nanocrystals with efficient up-conversion fluorescence. *Adv. Funct. Mater.* **2006**, *16*, 2324–2329.
25. Liu, C. H.; Chen, D. P. Controlled synthesis of hexagon shaped lanthanide-doped LaF<sub>3</sub> nanoplates with multicolor upconversion fluorescence. *J. Mater. Chem.* **2007**, *17*, 3875–3880.
26. Vetrone, F.; Mahalingam, V.; Capobianco, J. A. Near-infrared-to-blue upconversion in colloidal BaYF<sub>5</sub>:Tm<sup>3+</sup>,Yb<sup>3+</sup> nanocrystals. *Chem. Mater.* **2009**, *21*, 1847–1851.
27. Mahalingam, V.; Vetrone, F.; Naccache, R.; Speghinib, A.; Capobianco, J. A. Structural and optical investigation of colloidal Ln<sup>3+</sup>/Yb<sup>3+</sup> co-doped KY<sub>3</sub>F<sub>10</sub> nanocrystals. *J. Mater. Chem.* **2009**, *19*, 3149–3152.
28. Chen, G. Y.; Zhang, Y. G.; Somesfalean, G.; Zhang, Z. G.; Sun, Q.; Wang, F. P. Two-color upconversion in rare-earth-ion-doped ZrO<sub>2</sub> nanocrystals. *Appl. Phys. Lett.* **2006**, *89*, 163105.
29. Wang, F.; Liu, X. Upconversion multicolor fine-tuning: Visible to near-infrared emission from lanthanide-doped NaYF<sub>4</sub> nanoparticles. *J. Am. Chem. Soc.* **2008**, *130*, 5642–5643.
30. Qian, H. S.; Zhang, Y. Synthesis of hexagonal-phase core-shell NaYF<sub>4</sub> nanocrystals with tunable upconversion fluorescence. *Langmuir* **2008**, *24*, 12123–12125.
31. Yang, J.; Zhang, C. M.; Peng, C.; Li, C. X.; Wang, L. L.; Chai, R. T.; Lin, J. Controllable red, green, blue (RGB) and bright white upconversion luminescence of Lu<sub>2</sub>O<sub>3</sub>:Yb<sup>3+</sup>/Er<sup>3+</sup>/Tm<sup>3+</sup> nanocrystals through single laser excitation at 980 nm. *Chem. Eur. J.* **2009**, *15*, 4649–4655.
32. Bai, X.; Song, H. W.; Pan, G. H.; Lei, Y. Q.; Wang, T.; Ren, X. G.; Lu, S. Z.; Dong, B.; Dai, Q. L.; Fan, L. Size-dependent upconversion luminescence in Er<sup>3+</sup>/Yb<sup>3+</sup>-codoped nanocrystalline yttria: Saturation and thermal effects. *J. Phys. Chem. C* **2007**, *111*, 13611–13617.
33. Mai, H. X.; Zhang, Y. W.; Sun, L. D.; Yan, C. H. Highly efficient multicolor up-conversion emissions and their mechanisms of monodisperse NaYF<sub>4</sub>:Yb,Er core and core/shell-structured nanocrystals. *J. Phys. Chem. C* **2007**, *111*, 13721–13729.
34. Shan, J.; Ju, Y. Controlled synthesis of lanthanide-doped NaYF<sub>4</sub> upconversion nanocrystals via ligand induced crystal phase transition and silica coating. *App. Phys. Lett.* **2007**, *91*, 123103.
35. Liu, Z.; Yi, G.; Zhang, H.; Ding, J.; Zhang, Y.; Xue, J. Monodisperse silica nanoparticles encapsulating upconversion fluorescent and superparamagnetic nanocrystals. *Chem. Commun.* **2008**, 694–696.
36. Li, Z. Q.; Zhang, Y.; Jiang, S. Multicolor core/shell-structured upconversion fluorescent nanoparticles. *Adv. Mater.* **2008**, *20*, 4765–4769.
37. Hebbink, G. A.; Stouwdam, J. W.; Reinoudt, D. N.; van Veggel, F. C. J. M. Lanthanide(III)-doped nanoparticles that emit in the near-infrared. *Adv. Mater.* **2002**, *14*, 1147–1150.
38. Sivakumar, S.; van Veggel, F. C. J. M.; Raudsepp, M. Bright white light through up-conversion of a single NIR source from sol-gel-derived thin film made with Ln<sup>3+</sup>-doped LaF<sub>3</sub> nanoparticles. *J. Am. Chem. Soc.* **2005**, *127*, 12464–12465.
39. Wang, M.; Mi, C. C.; Wang, W. X.; Liu, C. H.; Wu, Y. F.; Xu, Z. R.; Mao, C. B.; Xu, S. K. Immunolabeling and NIR-excited fluorescent imaging of HeLa cells by using NaYF<sub>4</sub>:Yb,Er upconversion nanoparticles. *ACS Nano* **2009**, *3*, 1580–1586.
40. Kim, W. J.; Nyk, M.; Prasad, P. N. Color-coded multilayer photopatterned microstructures using lanthanide (III) ion co-doped NaYF<sub>4</sub> nanoparticles with upconversion luminescence for possible applications in security. *Nanotechnology* **2009**, *20*, 185301.
41. Wang, F.; Han, Y.; Lim, C. S.; Lu, Y.; Wang, J.; Xu, J.; Chen, H.; Zhang, C.; Hong, M.; Liu, X. Simultaneous phase and size control of upconversion nanocrystals through lanthanide doping. *Nature* **2010**, *463*, 1061–1065.